J. Membrane Biol. 116, 117–128 (1990)

The Journal of
Membrane Biology

Structural and Developmental Differences between Three Types of Na Channels in Dorsal Root Ganglion Cells of Newborn Rats

Ariela Schwartz, Yoram Palti, and Hamutal Meiri*
The Department of Physiology and Biophysics, Faculty of Medicine, and The Rappaport Family Institute for Research in the Medical Sciences, Technion—Israel Institute of Technology, POB 9697, Haifa, 31096, Israel

Summary. The changes in Na current during development were studied in the dorsal root ganglion (DRG) cells using the whole-cell patch-clamp technique. Cells obtained from rats 1–3 and 5–8 days after birth were cultured and their Na currents were compared. On top of the two types of Na currents reported in these cells (fast-FA current and slow-S current) a new fast current was found (FN). The main characteristics of the three currents are: (*i*) The voltages of activation are −37, −36 and −23 mV for the FN, FA and S currents, respectively. (*ii*) The activation and inactivation kinetics of FN and FA currents are about five times faster than those of the S current. (*iii*) The voltages at which inactivation reaches 50% are −139, −75 and −23 mV for the FN, FA and S currents, respectively.

The kinetics and voltage-dependent parameters of the three currents and their density do not change during the first eight days after birth. However, their relative frequency in the cells changes. In the 1–3 day-old rats the percent of cells with S, FA, and mixed S + FN currents is 22, 18, and 60% of the cells, respectively. In the 5–8 day-old, the percent of cells with S, FA, and FN + S is 10, 66 and 22%. The relative increase in the frequency of cells with FA current during development can contribute to the ease of action potential generation compared with cells with FN currents, which are almost completely inactivated under physiological conditions. The predominance of FA cells also results in a significant decrease in the relative frequency of cells with the high-threshold, slow current.

Antibodies directed against a part of the S_4 region of internal repeat I of the sodium channel (C_I^+, amino acids 210–223, eel channel numbering) were found to shift the voltage dependence of FA current inactivation (but not of FN or S currents) to more negative potentials. The effect was found only when the antibodies were applied externally. The results suggest that FN, FA and S types of Na currents are generated by channels, which are different in the topography of the C_I^+ region in the membrane.

Key Words Na channels · antibodies to synthetic peptides · patch clamp · action potential · ion channel development · sensory neurons

Introduction

The peripheral sensory system transduces sensory stimuli into electrical impulses and transmits them to the CNS [16]. The information regarding stimulus duration and intensity is encoded in a large repertoire of firing patterns [16, 22]. Usually neurons cannot produce the entire spectrum of firing. Rather, it seems that individual neurons specialize in generating a relatively narrow range of firing patterns [18, 19]. The specific firing patterns a neuron is capable of generating are dictated by the characteristics and relative abundance of its voltage-dependent ion channels. These parameters determine the firing threshold, rate of rise and duration of the action potential as well as the refractory period, accommodation, the ability to follow high frequency stimulation, and the ability to respond repetitively to a sustained stimulus [16, 22, 35].

The acquisition of voltage-sensitive ion channels by the cell membrane during development provides it with its typical firing pattern. Developmental changes in the composition of the various ionic channels and in their properties are reflected in changes in the firing patterns of individual neurons [44, 57] during development.

The sensory neurons of mammalian dorsal root ganglia (DRG) were found to have at least two types of voltage-dependent sodium channels: fast, TTX-sensitive (F) and slow, TTX-resistant (S) [30, 35, 38, 46, 47, 65]. Action potential measurements implied that the proportion of neurons with "pure" F channels (completely blocked by TTX) is increased from newborn to adult. This observation indicates the need to follow developmental changes in the ion channels themselves.

In this study the properties of the individual channels were examined, and the compositions of Na channels among neurons during development

* *Present address:* C/O Prof. E.M. Landau, Department of Psychiatry, Room 3F-02, VA Hospital, 130 Kingsbridge Rd., Bronx, New York 10468.

were measured by the whole-cell patch-clamp technique [17]. The dorsal root ganglion cells were cultured from 1–8 day-old rats for 2–6 hr.

The particular questions we asked were: What Na currents are present during the first eight days after birth? Have their properties changed during this period? Have their relative frequency in the neurons changed? And is there a structural basis for the differences between Na channels responsible for the three currents? To answer the last question, an immunological approach was employed.

Materials and Methods

Generation and Characterization of Anti-C_I^+

A peptide corresponding to amino acids 210–223 (eel channel numbering [43]), termed C_I^+, was synthesized by the solid phase method of Merrifield [39] and purified as previously described [37, 38]. The peptide was conjugated to carrier proteins for immunizing rabbits [37, 38]. The immunoglobulin fractions from whole anti-C_I^+ serum or pre-immune serum were purified on a Protein A column. Antibodies were further adsorbed to liver membranes [37] to eliminate the nonspecific components.

ELISA was used to quantify immunoglobulin content in a given preparation or to measure the binding of anti-peptide antibody to the peptide as well as to various membranes, and purified preparation [37, 38]. Further characterization of the immunochemical interaction between anti-C_I^+ and Na channels was described elsewhere [37].

Cultures of Dorsal Root Ganglion (DRG) Cells

Ganglia were isolated from 1–8 day-old rats, and transferred into CMF solution (136.8 mM NaCl, 2.6 mM KCl, 0.28 mM Na_2HPO_4, 2.6 mM $NaHCO_3$, 33.3 mM glucose, pH 7.4 supplemented with 100 U/ml penicillin, 0.1 mg/ml streptomycin and 12.5 U/ml nystatin). Ganglia were incubated for 20 min at 37°C with trypsin (0.05% Difco, 1 : 250). The enzyme was washed-out with culture medium. The medium was Eagle's basal medium supplemented with 5% fetal calf serum, 2 mM glutamine, 0.3% glucose, and antibiotics (*as above*) (all supplied by Beit Haemek, Israel). In several cases, the trypsin step was omitted. Single cell suspension was produced by trituration with flame-polished Pasteur pipette.

Cells (10^3–10^4) were seeded on poly-L-lysine-coated petri dishes with 1.5-ml culture medium. Cultures were incubated for 2–6 hr at 37°C.

Neurons (10–15 μm in diameter) were distinguished from Schwann cells by their round shape, bright halo and short, thin neurites. All studies described here relate only to the subpopulation of cells of the said size and shape.

Electrophysiological Methods

Solutions

Extracellular solution consisted of 110 mM NaCl, 2.5 mM $MgCl_2$, 5 mM KCl, 40 mM tetraethylammonium (TEA) chloride, 5 mM HEPES, 2 mM Na_2HPO_4, 100 μm $CaCl_2$, 10 mM glucose, pH 7.4, adjusted with NaOH and osmolarity adjusted to 300 mosM. The perfusion system enabled changes in the composition of the external solution within 3 min.

Fire-polished borosilicate electrodes (2–3 MΩ, 1–2 μm in external diameter) were filled with the internal solution consisting of 120 mM CsCl, 2.5 mM $MgCl_2$, 10 mM NaCl, 5 mM KCl, 5 mM HEPES, 5 mM EGTA, pH 7.4 adjusted with CsOH. Osmolarity was adjusted to 280–290.

Potassium currents were blocked by TEA from the outside and Cesium ions from the inside. Blocking of calcium currents was achieved here by a combination of three components: (*i*) magnesium (2.5 mM) on both sides of the membrane [1, 9, 20, 26]; (*ii*) calcium (10 μm) in the external solution [9, 20, 26, 29]; and (*iii*) EGTA (5 mM) in the internal solution [1, 9]. Other pharmacological methods of blocking of calcium channels were not effective in this preparation [1, 9, 26, 29, 47].

Electrophysiological Setup

The experiments were carried out using a List pre-amplifier, EPC-7, with 1-GΩ head-stage set for the whole-cell patch-clamp configuration [17]. Capacitive transients were minimized using the List control on-line [17] and were further reduced by a proportional subtraction of transients elicited at the termination of a pulse from −150 to −70 mV. To ensure adequate space clamp, cells without processes or with thin (1–2 μm) processes, no longer than twice the cell diameter, were selected. All recordings were performed at room temperature (24 ± 1°C).

The cells were held at V_m of −70 mV. A Data General "Desk Top-30" computer with analog-to-digital and digital-to-analog converters were used to generate command voltages at 3-sec intervals, and to digitize the currents at sampling rates of 2–24 kHz at 10-bit resolution. All currents were low-pass filtered at 10 kHz.

The leakage conductance (g_L) was determined from a hyperpolarizing pulse, and the leakage current (I_L), for any pulse potential, was calculated assuming that g_L does not vary with membrane potential and that I_L is reversed at −70 mV. Experiments in which the leakage conductance exceeds 5% of maximal Na conductance were rejected.

Attenuation of I_{Na} by TTX did not result in a shift of the current-voltage ($I - V$) relationship along the voltage axis, indicating that the series resistance error was negligible [49, 58]. Indeed, any attempt to correct for series resistance initiated oscillations.

Separation of Sodium Currents

Protocols designed to separate between fast and slow Na currents were adopted from Zeitoun et al. [65] and are described here briefly. Na currents of DRG cells can be separated into low-threshold fast currents and high-threshold slow currents. These currents also differ in the voltage dependency of their inactiva-

tion function. At the termination of a 40-msec conditioning potential of −50 mV, the fast currents are completely inactivated, and the slow current is practically fully activated. In contrast, when depolarization is given at the termination of a conditioning prepulse to −150 mV, both fast and slow currents are activated. On the basis of these differences two pulse protocols were given to obtain the $I - V$ curve. In MF protocol the conditioning potential was −150 mV, and in MS protocol it was −50 mV. The 40-msec conditioning prepulse was given from the holding potential (−70 mV) and was followed by 40-msec test pulses to various V_m values between −70 and +80 mV, in 5 to 10-mV increments. The series of command pulses were identical in both protocols.

Relative Conductance $\{g_{Na}/g_{Na(max)}\}$

The sodium conductance at the time of the peak current $\{g_{Na}\}$, at each V_m, was calculated from $g_{Na} = I_{peak}/(V_m - E_r)$ where E_r is the current reversal potential. The g_{Na} at each V_m was then normalized to the largest g_{Na} ($g_{Na(max)}$), and the normalized values (i.e., the relative conductances) were plotted against V_m.

Steady-State Inactivation Curve $\{I_{Na}/I_{Na(max)}\}$

Based on the 30–40 mV shift between the relative conductance curves of the fast currents and the slow current, two inactivation protocols were designed. In the HF protocol, cells were given 40-msec prepulses to various V_m values (V_{pp}) between −160 and −30 mV, in 10-mV increments. The prepulses were followed by a 40-msec test depolarization to −25 mV, i.e., to a membrane potential where the slow currents are barely activated. In the HS protocol, prepulses were given to V_m between −100 and 0 mV. The prepulses were followed by a 40-msec pulse to $V_m = +5$ mV, i.e., a potential where all currents are significantly activated. In both protocols the inactivation is measured as the ratio between I_{peak} obtained following any prepulse potential, and the maximal I_{peak}.

Criteria for Defining Fast and Slow Cells

Pure S cells generated only S currents, regardless of the prepulse (−150 mV) used. Their current amplitude at a given depolarization was either unchanged by both −150 and −50 mV prepulses or at most increased by 10% by the −150 mV prepulse. The typical inactivation curve of a pure S cell was obtained only with the HS protocol, and no currents were initiated by the HS protocol.

A pure fast cell generated currents only when the prepulse was −150 mV. With a prepulse to −50 mV the fast current was 90–100% inactivated. The kinetics of the attenuated current were similar to those of the larger current obtained with the prepulse to −150 mV. The inactivation curve of a pure fast cell could be studied only with the HF protocol since fast currents were not elicited using the HS protocol.

Calculation of Time Constants

The time constant of inactivation (tau_h) was calculated at various V_m, from the slopes of $\log(I_t - I_{inf})$ *vs.* time relationships over the linear range, where I_{inf} is the current at the end of the 40-msec depolarizing pulse, I_t are the current values at any time t, following the peak current, where the log relationship is linear.

Time constant of activation (tau_m) was calculated at various V_m from the slopes of the $\log(I_{inf} - I_t)$ *vs.* time relationships in the region of linearity, where I_{inf} is the peak sodium current value and I_t are the current values at any time t, prior to the peak current, but not too close to the peak (where the log relationship deviates from linearity). Tau_m values incompatible with the upper frequency limit of the filter (10 kHz) were rejected.

Antibody Application

Extracellular application was achieved by adding the antibody to the externally perfusing solution at a concentration of 100 μg/ml. When an effect was established, it reached saturation within 15 min. Intracellular application was achieved by adding the antibodies (100 μg/ml) to the internal solution in the patch pipette. Measurements were taken immediately after the patch was formed and 25–30 min later. Our calculation indicated that the time required for a 150-kD protein (IgG) to approach equilibrium by diffusion into the neuron is about 20 min [27].

Results

Characterization of Three Types of Na Currents

Three types of Na currents can be identified in DRG cells of 1–8 day-old rats, as demonstrated in Figs. 1 and 2 and in Table 1. Two currents are fast, denoted FN and FA (for reasons explained below) and one current is a slow, S current. Both fast currents have rapid kinetics of activation and inactivation, about five times faster than Tau_h of the slow current (Table 1). This kinetic difference is the first criterion used to separate the slow from the fast currents.

The two fast currents are activated at significantly ($P < 0.001$) more negative membrane potentials: −37.7 ± 3.1 mV (FN) and −36.3 ± 7.9 mV (FA) in comparison to −23 ± 6.5 mV for the slow current (Table 1 and Fig. 2*A*). The $I - V$ curves of the two fast currents reach a peak at more negative membrane potentials −17.5 ± 4.8 mV (FN current) and −12.6 ± 5.9 mV (FA current, $P < 0.05$, for the comparison between the two fast currents using a two-tailed, t test). In comparison, the peak of the slow current is reached at −6.1 ± 4.6 mV (Table 1 and Fig. 2*A*).

All currents are reversed between 52 and 53 mV (Fig. 2*A*) i.e., approximately at the calculated E_{Na} (58 mV). The increase in channel conductance *vs.* membrane potential reaches 50% at −29.7 ± 3 mV (FN) and −26.5 ± 7.8 mV (FA) in comparison to

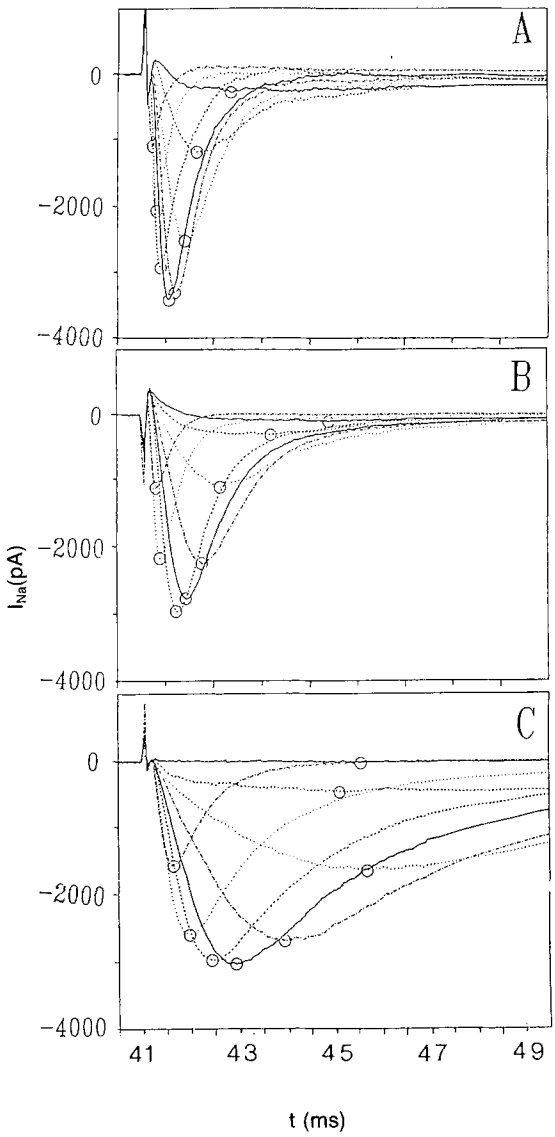

Fig. 1. Three types of Na currents: (*A*) fast newborn (FN); (*B*) fast adult (FA); and (*C*) slow (S) currents. The fast currents (*A* and *B*) were initiated by the MF protocol and the slow currents (*C*) by the MS protocol. Depolarization was to: −40, −35, −30, −20, −15, 0, +10, and +30 mV (*A*); −70, −40, −35, −30, −25, −15, −10, +15, and +40 mV (*B*); and −40, −20, −15, −10, −5, 0, +10, and +30 mV (*C*). Traces are shown after subtraction of leakage and capacity currents. Open circles: peak I_{Na}. The cells of *A*, *B* and *C* were taken from 1–3 day-old rats after being in culture 2 hr

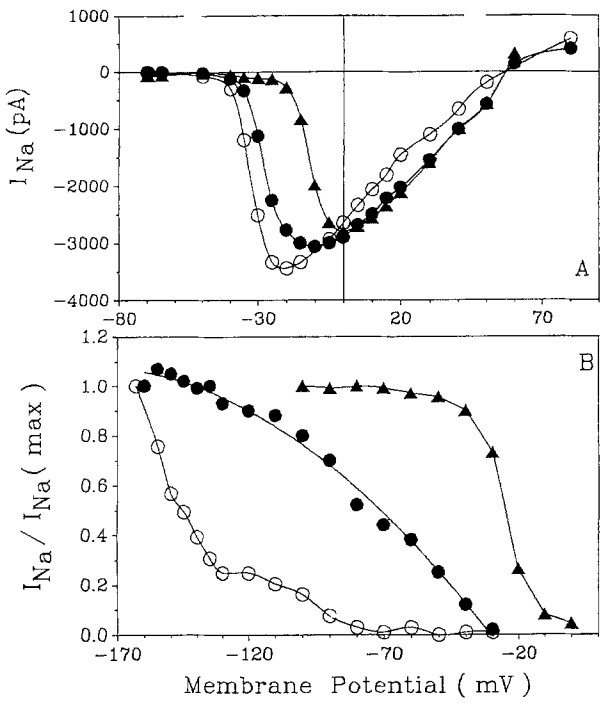

Fig. 2. (*A*) The $I - V$ curves of the three current types shown: FN current, open circles; FA current, filled circles; and S currents, filled triangles. (*B*) The inactivation [$I_{Na}/I_{Na(max)}$] curves of the three current types: FN, open circles, FA, filled circles; and S, filled triangles. The S curve was obtained using a test pulse to +5 mV (HS protocol). The FN and FA curves were obtained using a test pulse to −25 mV (HF protocol)

the higher value of −17.6 ± 4.6 mV for the S current ($P < 0.001$) (Table 1). Thus, in general, the two fast currents have a lower threshold and more rapid kinetics in comparison to the S current.

The main difference between the two fast currents is in their voltage-dependent inactivation. FN current is 50% inactivated at V_m = −139.1 ± 5.6 mV whereas FA current is 50% inactivated at V_m = −75.3 ± 8.1 mV ($P < 0.001$). The S current reached 50% inactivation at much higher depolarization, −23.5 ± 5.3 mV. The difference in inactivation is also expressed in the shape of the entire inactivation curve. The curve of S current inactivation has the typical steep, inverse S-shape (Fig. 2*B*). The FA inactivation curve is far less steep (Fig. 2*B*). The inactivation of FN current has an unusual shape: in the range of −(60–120) mV it has low dependence on V_m, whereas in the range of −(120–160) mV, the curve increases steeply with V_m. Prepulses to V_m more negative than −160 mV resulted in membrane breakdown. Therefore, the inactivation curve was arbitrarily normalized to the current value at −160 mV, although the curve did not tend towards saturation at this conditioning prepulse (Fig. 2*B*).

Developmental Changes of Na Currents

All three types of Na currents were found among DRG cells obtained from newborns during the first eight days after birth. The current amplitude (Table 2), the voltage dependence and kinetics of each cur-

Table 1. Three types of Na currents in DRG cells

Parameter	Current type		
	Fast newborn	Fast adult	Slow
Peak IV (mV)	−17.5 ± 4.8 (n = 10)	−12.6 ± 5.9** (n = 15)	−6.1 ± 4.6 (n = 13)
V activation (mV)	−37.7 ± 3.1 (n = 15)	−36.3 ± 7.9 (n = 19)	−23 ± 6.5 (n = 21)
E_{Na} (mV)	52.4 ± 7.1 (n = 15)	52.4 ± 7.8 (n = 19)	53.1 ± 5.8 (n = 21)
V_{h50} (mV)	−139.1 ± 5.6■ (n = 7)	−75.3 ± 8.1*** (n = 19)	−23.5 ± 5.3 (n = 20)
V_{g50} (mV)	−29.7 ± 3.0 (n = 4)	−26.5 ± 7.8 (n = 18)	−17.6 ± 4.6 (n = 20)
τ_h (msec) (at −10 mV)	1.11 ± 0.2 (n = 5)	0.98 ± 0.35 (n = 9)	6.7 ± 4.8 (n = 9)
τ_m (msec) (at −15 mV)	NT	NT	1.5 ± 0.1 (n = 4)

Values are mean ± SD. All values of slow current (except E_{Na}) are statistically different from those of fast adult and fast newborn currents ($P < 0.001$, two-tailed unpaired t test). Asterisks indicate differences between the two fast currents (*** $P < 0.001$, ** $P < 0.05$, two-tailed unpaired t test). NT, value not tested; ■, V_{h50} of FN current calculated from curves which were arbitrarily normalized to the current elicited by a prepulse to −160 mV, although the curve did not reach saturation there.

rent (*not shown*) do not change during this period. However, developmental changes are expressed in the relative frequency of these three currents among the DRG cells. It is important to emphasize that this relative frequency does not relate to all DRG cells but only to the 10–15 μm cells, before they sprout. Smaller cells were already reported to be pure S cells [5]. Larger cells could not be studied due to lack of space clamp.

In terms of currents' distribution, several types of cells were identified: pure S cells (generating only S current), pure FA cells (generating only FA current), and mixed cells, generating both FN + S currents, or FA + S currents. No pure FN cells were found under any set of conditions and test potentials.

Mixed cells (Fig. 3) generated currents composed of a mixture of FN + S or FA + S currents within a single cell. The presence of such a composition is clearly visible under the properly chosen set of conditions. For example, when a prepulse to −150 mV is followed by a test pulse to −30 mV, the resultant current has two peaks (inset of Fig. 3). If a similar test pulse is given following a prepulse to −50 mV, only the current corresponding to the late (slow) peak is generated (inset of Fig. 3). Subtracting the two traces one from another yields the trace corresponding to the early peak (inset of Fig. 3). Using this subtraction protocol, the slow currents in mixed cells can be separated from the fast currents. In addition, the separate inactivation curves for FN, FA and S could be obtained from mixed cells by employment of the HF and HS protocols.

Table 2. Developmental changes of Na current
A: Distribution of cells with current types

Age	S	FN	FA	FN + S	FA + S
1–3 days (n = 21)	23.8%	0	14.3%	52.4%	9.5%
5–8 days (n = 45)	10%	0	66%	22%	2%

B: Peak current density (nA)

Age	S	FN	FA	FN + S	FA + S
1–3 days (n = 21)	2.5 ± 1.1 (n = 5)	—	3.8 ± 1.5 (n = 3)	3.3 ± 1.6 (n = 11)	1.25 ± 2.46 (n = 2)
5–8 days (n = 26)	2.1 ± 0.4 (n = 3)	—	2.7 ± 1.2 (n = 19)	2.37, 3.4 (n = 2)	1.60, 1.43 (n = 2)

A: Frequency of cells with different types of currents. S, pure slow currents; FN, pure fast newborn current; FA, pure fast adult current; FN + S and FA + S, cells with mixtures of the above.
B: Peak current amplitude of 10- to 15-μm cells having different types of currents. As all cells are of the same diameter and all have no neurites, the similar current amplitude indicates similar current density.

It was found that using DRG cells from 1–3 day-old rats, 22% of the cells are pure S cells, 18% of the cells are pure FN cells, and 60% are mixed

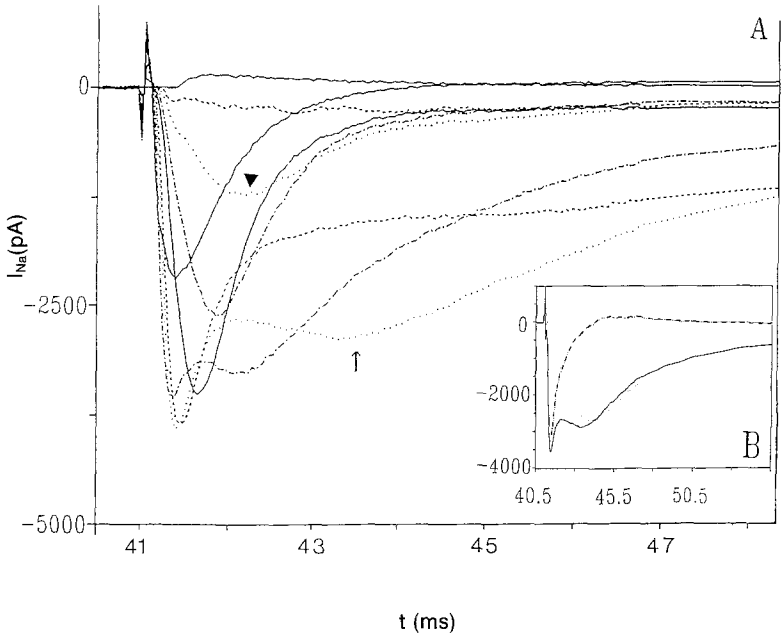

Fig. 3. (*A*) Mixed FN + S currents in a single cell. Currents were initiated by the MF protocol. Traces are shown for depolarizations to: −45, −35, −25, −15, −5, and +20 mV. At the depolarization to V_m = −35 mV (arrow head) only the FN current is visible. At the depolarization to V_m = −25 mV (arrow) two peaks are seen: the early peak corresponds to the FN current, and the late peak corresponds to the S current. (*Inset*) Three currents initiated by a test depolarization to V_m = −25 mV. Solid line: combined current generated following a prepulse to −150 mV. Dotted line: the slow current generated following a prepulse to −50 mV. Dash-dotted line: the fast current obtained by subtracting the slow from the combined current

FN + S cells (Table 2). In DRG cells from 5–8 day-old rats only 10% of the cells are pure S cells, and 66% of the cells are pure FA cells. The rest (22%) are mixed cells having FN + S currents (Table 2). There were only two cells with FA + S currents (Table 2). Of the two fast currents, the one called FN was predominately found in cells from newborns whereas the FA current predominates in cells from 5–8 day-old (and adult rats [35]). The slow current, which is present in 82% of the cells in 1–3 day-old rats (either in its pure form or in a mixture with FN current), becomes less frequent in the 5–8 day population (all together: 34%). Note that in adults, action potential corresponding to the presence of slow currents are found in less than 20% of the cells [34, 64].

Another major difference between the two age groups was in the decreased frequency of FN current (60% of the cells in 1–3 day-old rats in comparison to 22% in 5–8 day-old rats), and the increased frequency of the FA current (from 18% of the cells in 1–3 day-old to 68% of the cells in 5–8 day-old rats). The only parameter in which FN and FA currents are actually different is Na inactivation. Thus, cells with FA current are more likely to fire action potential than cells with the FN current, which are inactivated under most physiological conditions. The increased frequency of FA cells over cells with FN currents, is predicted to be accompanied by an increased contribution of the fast current to firing patterns of DRG cells. The corresponding decreased frequency of S *vs.* FA currents suggests, that during the period from 1–3 to 5–8 days after birth there is a decrease in the proportion of cells which require strong stimulus to initiate firing.

Searching for a Structural Basis for the Differences between the Channels

To gain insight into the potential structural differences between the three current types, an immunological approach was taken. Since the three currents mainly differ in their voltage-dependent inactivation, antibodies that were shown to shift the inactivation function on the voltage axis [37, 38] were chosen as molecular probes. These antibodies were raised against a part of the S_4 segment of internal repeat I of Na channel designated C_I^+ (Fig. 4). This segment is considered to participate in voltage-dependent processes of Na channel gating [42, 59].

It can be seen in Fig. 5*A* and Table 3 that when applied externally the only significant effect of the antibodies was to shift the inactivation curve of FA current towards more negative membrane potentials, without shifting the relative conductance *vs.* membrane potential curve. The effect, which developed within 10–15 min, was expressed in a mean shift of 25.8 ± 5.8 mV as compared to the 9.25 ± 6.4 mV shift produced by IgG of pre-immunized rabbits (Fig. 5*A* and *B* and Table 3). There was no parallel effect of anti-C_I^+ on the FN and S currents (Table 3). Anti-C_I^+ and the control IgG-modified FA current in DRG cells, regardless of the postnatal day (*not shown*). However, the FA current was rare on postnatal days 1–3 (Table 2). Thus, with the limited

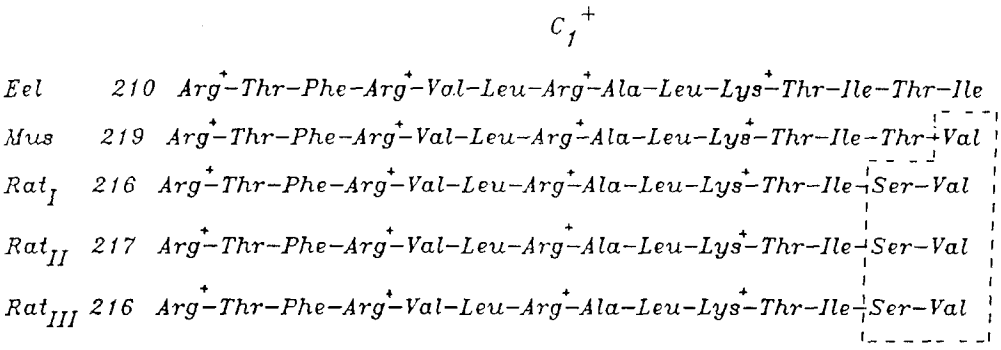

Fig. 4. C_I^+ synthetic peptide sequence made according to eel electroplax Na channel [43] and its corresponding regions in three sequenced Na channels of rat brain (R_I, R_{II} and R_{III}) [28, 42] and skeletal muscle Na channel [61]. Dashed line the nonconserved amino acids

Table 3. Current modification by antibodies

I_{Na} type	Antibody	Side of membrane	Peak I_{Na} left (%)	V_{h50} (mV)	V_{g50} (mV)	E_{Na} (mV)	Tau_h msec
FA	Anti-C_I^+	Outside	82.3 ± 16.7 (n = 6)	25.8 ± 5.8 (n = 5)[a]	3.1 ± 1.1 (n = 6)	0.125 ± 0.09 (n = 4)	5 ± 0.8 (n = 4)
	NR-IgG	Outside	88.2 ± 10.6 (n = 7)	9.25 ± 6.4 (n = 8)	2.5 ± 2.9 (n = 6)	0.125 ± 0.15 (n = 4)	2.6 ± 2.5 (n = 3)
	Anti-C_I	Inside	89.39 (n = 2)	3.3 ± 2.8 (n = 3)	0 (n = 3)	NT	53 ± 4.1 (n = 3)
	NR-IgG	Inside	72.8 (n = 2)	5 (n = 1)	2 (n = 1)	NT	3 (n = 1)
	EG-100	—	85 ± 10 (n = 5)	6 ± 4 (n = 5)	1 ± 0.5 (n = 5)	0 (n = 5)	2 ± 1 (n = 5)
S	Anti-C_I^+	Outside	67 ± 15.5 (n = 11)	6.8 ± 4.7 (n = 11)	2.8 ± 2.5 (n = 9)		5.4 ± 4.2 (n = 7)
	NR-IgG	Outside	70 ± 17.4 (n = 4)	9.1 ± 3.4 (n = 6)	1.2 ± 2.1 (n = 5)		1, 0.8 (n = 3)
	Anti-C_I	Inside	64 ± 29.4 (n = 8)	3.1 ± 2.8 (n = 9)	3.3 ± 2.5 (n = 8)		1.3 ± 4.2 (n = 8)
	NR-IgG	Inside	74 (n = 2)	7.3 (n = 2)	3.2 (n = 2)		0.0 (n = 2)
	EG-100	—	70 ± 10 (n = 4)	2 ± 1 (n = 4)	1 ± 0.5 (n = 4)	0 (n = 4)	1 ± 0.4 (n = 4)
FN	Anti-C_I^+	Outside	60 ± 18 (n = 4)	0.2 ± 0.4 (n = 5)	3, 0 (n = 2)	NT	2.4 ± 1.3 (n = 5)
	NR-IgG	Outside	62 (n = 1)	0 (n = 1)	2 (n = 1)	NT	2 (n = 1)
	Anti-C_I	Inside	100, 80 (n = 2)	0.6 ± 0.9 (n = 3)	3, 0 (n = 2)	NT	1, 3 (n = 2)
	EG-100	—	65 ± 10 (n = 4)	0.3 ± 0.2 (n = 3)	2 ± 1 (n = 4)	0 (n = 4)	1.5 ± 0.5 (n = 3)

FA, FN and S are fast adult, fast newborn and slow currents, respectively. Anti-C_I^+ and NR-IgG are the IgG fractions of the anti-serum to C_I^+ and the nonimmunized rabbit serum. EG-100 is normal external physiological solution. All values are means ± SD.
[a] $P < 0.01$ in two-tailed t test (comparison between anti-C_I^+ and NR-IgG when both were given externally).

number of cells available for examination, our conclusion is that the effect of the antibody on the FA current most probably does not change during postnatal development.

The effect of control (pre-immune) IgG was specific. Neutral proteins, such as casein and BSA, when employed at a similar concentration (100–200 μg/ml), had no effect on inactivation (*data not*

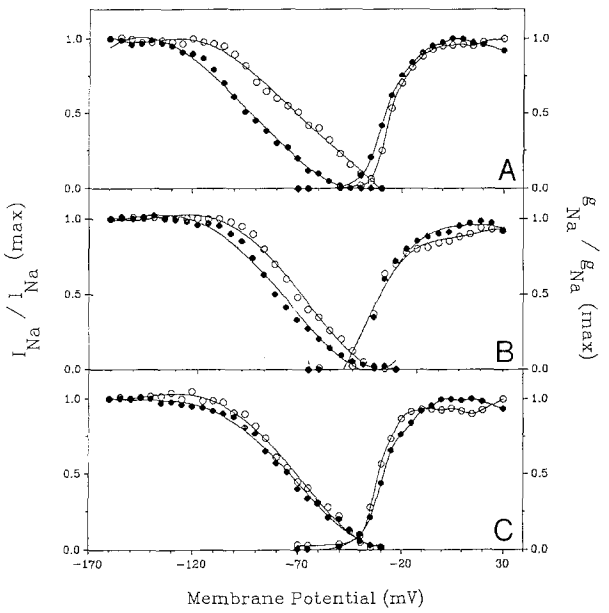

Fig. 5. (*A* and *B*) The steady-state inactivation [$I_{Na}/I_{Na(max)}$] and relative conductance [$g_{Na}/g_{Na(max)}$] *vs.* membrane potential, of three FA cells. Empty circles before and filled circles: 20 min after exposure to 100 μg/ml of antibody. In *A* and *B* antibodies were applied by external perfusion. *A*: exposure to anti-C_I; and *B*: normal rabbit IgG (NR-IgG). (*C*) The antibodies were added to the internal solution and applied via the pipette. Empty circles: measurements made immediately after establishing the seal (control). Filled circles: measurements made 25 min later

shown). One way to explain the effect of control IgG is to attribute their effect to their electric charges, which may electrostatically influence Na channel inactivation [37].

The results indicate that the region corresponding to the C_I^+ domain of the Na channel is present in the FA channel molecules and is accessible to antibodies at the external surface of the membrane. This domain is either missing, inaccessible, or not associated with any function in the FN and S channels.

Discussion

Three Types of Na Currents in Rat DRG Cells

The diversity of Na currents in DRG cells of newborn rats is expressed by the presence of three well-characterized Na currents: the fast adult (FA), the fast newborn (FN), and the slow (S) currents. The FA and S currents were previously described in DRG cells of 7- to 10-day-old rats [30, 38] and in adult rats [35]. The FN current has been described in detail here for the first time. This current is almost completely inactivated without a conditioning hyperpolarizing prepulse to membrane potentials below −120 mV. This might be the reason why this current was not detected in previous studies, which did not utilize such strong hyperpolarizing prepulses [30, 35, 46, 47].

Our experimental approach was designed to avoid modification of the ionic channels. The measurements were made as soon as possible after removal of the ganglia from the body. Controls, previously performed in our laboratory [46], showed that trypsinization of the DRG cells does not elicit new Na currents nor modify the existing Na currents. We can therefore conclude that the three Na currents are the natural currents of DRG cells [32, 52].

The differences in current properties are most probably responsible for the differences in firing patterns. The action potentials of cells with FA current rise rapidly, are of short duration, and have a low firing threshold [21, 34, 35, 45, 55, 65]. These cells can follow high-frequency stimulation, but respond only once or twice to a sustained depolarization [35]. The action potentials of cells with S current rise slowly, are of long duration, and have a high threshold [34, 35, 55, 64]. These cells fire repetitively in response to a sustained depolarization [35]. The higher thresholds for activation of S current *vs.* the FA and FN currents may account for the higher stimulus required to fire a slow action potential. The slow inactivation kinetics of S *vs.* FA and FN currents explains why a sustained depolarization produces a train of action potentials in S cells, whereas cells with FN and FA currents are rapidly inactivated.

The difference in the inactivation voltage between FN and FA cells had an important effect on their excitability: cells with FA currents may generate action potential under a variety of physiological conditions under which cells with the FN currents are expected to be completely inactivated. It has been shown that the resting potentials of DRG cells are similar, regardless of the current they express [45, 47]. Thus, it is hard to imagine physiological conditions under which cells with only FN current can generate action potentials. In fact, it is anticipated that if an action potential is elicited by a cell with FN current, it must have either a very low K conductance or an n_∞ curve strongly shifted towards depolarization [22, 24]. It is interesting that, in nature, the problem is usually bypassed, as the FN current is found in cells together with the S current, and the latter can lead to firing of action potentials under a variety of physiological conditions [35, 45, 64].

Developmental Changes in Na Currents of Rat DRG Cells

In newborn rats the characteristics of each current do not change during the first postnatal days. Furthermore, we have not found an increase in Na current density, as was found in developing frog neurons [15, 44]. What does change, during the development of rat DRG cells, is the percent of cells expressing pure FA, S, and FN currents or their combinations. Note that the said results could be quantitative rather than qualitative, as the amplitude of some currents may simply fall below resolution of our measurements. In postnatal development, the proportion of neurons with FA current decreases, whereas the proportion of neurons with FA current increases. This process probably continues, since in adult rats the S current in the population of cells 10–15 μm in diameter is very small [34, 35, 64]. The impact of such developmental changes on the proportion of neurons with different firing patterns was discussed above and is consistent with previous reports [34, 35, 64].

Several mechanisms may be responsible for the developmental changes described in this study.

Age-Dependent Changes

The DRG cells are born on embryonic day 16, and their number is greatly increased between days 16 and 18 [15, 51]. Thus, there are more mature cells on postnatal days 5–8 than on postnatal days 1–3. Matsuda et al. [34] and Yoshida et al. [64] have already shown a reduction in the frequency of cells with slow action potential during postnatal development. On the basis of our results, one can predict that young cells would have FN and S currents, whereas maturation would be associated with an increase in FA cells. This assumption nicely fits the results of this study. However, other studies performed in our laboratory [65] and elsewhere [21] have shown that most freshly isolated DRG cells from 16-day embryos have FA current, whereas S current is rare and FN current is not found. Thus, the age factor alone cannot provide a full explanation for the developmental changes we found between postnatal days 1–3 and 5–8.

Target Influence

The target (whether peripheral or central) can influence channel properties and number. This has been shown by the effect of NGF (a factor released in nature by the peripheral target tissue) on channel number and distribution [8, 10, 33, 36, 46, 51]. Innervation has also been found to influence the number of F *vs.* S channels in muscles [63]. In our case a scenario which can fit the results involves the presence of a large density of FN *vs.* S currents on embryonic day 16 (before innervation), which is reversed upon innervation (newborn) but recovered during synaptic elimination (postnatal days 7–10). The validity of such a scenario remains to be tested.

Switching, Shutting Down, or Recruiting Channels

It is easy to imagine how FN can be switched with FA current, and vice versa, as the only difference between them is the voltage dependency of the inactivation. Different levels of phosphorylation [6], oxidation [25, 48, 56], or modification of arginine or lysine residues [7, 41] can produce such a change. In the same context, oligomerization of the beta with the alpha subunits of the channel can accelerate channel kinetics and increase TTX sensitivity—a process which can account for a switch from S to FA current [31, 40, 54]. However, the differences between current proportions can be a reflection of the replacement of one channel subunit with another (as in the nicotonic cholinergic receptor channel [53]). Channel subtypes can also be recruited by a second messenger [4, 6].

Structural Basis for the Differences between the Na Channels Generating the Three Types of Currents

To elucidate the structural basis for the difference between current types, an immunological approach was employed. The antibodies denoted anti-C_I^+, directed against the most conserved element of the Na channel—the S_4 segment [28, 42, 43, 61]—were found to shift the voltage-dependent inactivation of the FA (but not the FN or S) current to more negative membrane potentials. The antibody works from the external, but not from the internal, surface of the membrane. These results suggest that in the channel eliciting the FA current, the region corresponding to C_I^+ is associated with the voltage sensor [3] of inactivation and is accessible from the external medium.

The anti-C_I^+ effect may be a specific steric hindrance, due to its binding with the channel [22, 23]. Effects of the IgG electric charges [3, 23, 37] can also be involved.

The C_I^+ domain is the most conserved (86–95%) part of the Na channel molecule (Fig. 4) [42, 61]. In

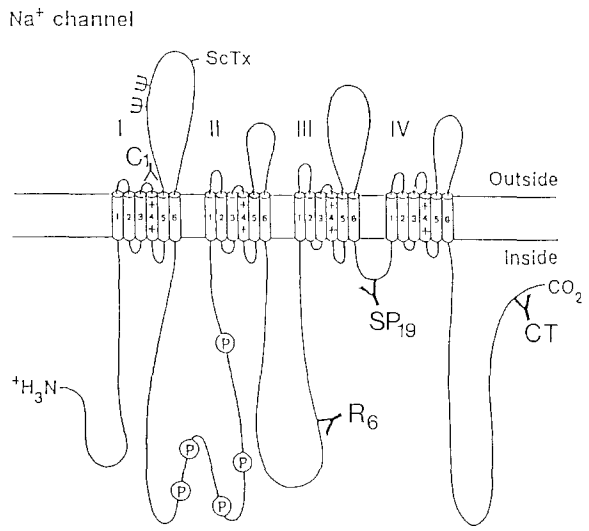

Fig. 6. Schematic model of Na channel domain associated with inactivation. *I–IV*: the internal repeats [42, 43]. SP_{19} region [59, 62] associated with kinetics of Na channel inactivation. *P*: The internal phosporylation region between repeats I and II, with five phosphosylation sites [6, 11]. The site for alpha-scorpion toxins (*ScTx*) between S_5 and S_6 of repeat I [6]. *CT*: C terminal region [13]; R_6: cytoplasmic region [14]. The C_1^+ region is pointed. Pluses on S_4 segments: the voltage sensor [59]. (Modified from ref. 6]

fact, such a domain has been found in all voltage-activated ionic channels [50, 60]. However, whereas the principal structure of this region is preserved (namely, the arrangement of a positively charged amino acid in each third position, with two neutral residues intervening), the actual sequence in the voltage-sensitive K channels [50] or the DHP receptor of Ca channels [60] is different. Thus, it is most unlikely that sequence differences [12, 37, 42, 43, 61] can account for the lack of anti-C_1^+ modification of FN and S currents. A more probable explanation would be tertiary structural differences.

Another explanation can be a difference in the availability of the C_1^+ domain to antibodies, due to different orientation of this segment in the membrane.

Finally, as mentioned above, chemical modification (oxidation, lysine or arginine neutralization, etc.) may account for the differences between the channels [6, 7, 25, 41, 48] and affect the ability of the antibodies to recognize their sites [37].

Stuhmer et al. [59] found that replacing a lysine in the C_1^+ region of rat II Na channel [42] with a neutral amino acid (glutamine) shifted the voltage-dependent Na channel activation along the voltage axis. Furthermore, its replacement with a negatively charged amino acid (glutamate) changed the slope of activation *vs.* membrane potential curve. Two-point mutations were accompanied by larger effects. In our study, Na channel activation was not altered by the antibodies. This may be attributable to the fact that the amino acids involved in activation are localized in a region inaccessible to antibodies, whereas regions involved in inactivation are closer to the external surface of the membrane [Fig. 6]. Aldrich et al. [2] suggested that inactivation is the last step in the cascade of the channel gating. Thus, a small effect of the antibodies on more than one step may become significant only on the last step in the cascade [22].

Four parts of the Na channels are now known to be involved in inactivation (Fig. 6): (*i*) the intracellular region between internal repeats III and VI (sp_{19}, Fig. 6) [59, 62]; (*ii*) the cytoplasmatic region between internal repeats II and III, which in rat brain carries four or five phosphorylation sites [6, 11]; (*iii*) the extracellular region between segments 5 and 6 of repeat I, which has been identified as the site for *Leiurus* toxin binding and sea anemone binding [6]; and (*iv*) the C_1^+ region (at least its externally facing side), which is not very far from the ScTx site. The inactivation-related sites for batrachotoxin and local anesthetics have not been localized to date [4, 6, 22]. Obviously, more sodium channel-specific antibodies and mutants are required to provide the complete picture of the domains involved in sodium channel activation and inactivation.

We are grateful to Dr. I. Zeitoun, who helped us apply the pulse protocols; to Dr. M. Sammer for the preparation and purification of anti-C_1^+, to Drs. R. Schatzberger and Y. Rosenthal for their useful advice, and to the Computer Center team for their great help. This work was supported by grant 84-00367 from the U.S.-Isreal Binational Science Foundation and by grant 480.87 from the Basic Research Fund administered by the Israel Academy of Sciences and Humanities.

References

1. Aldrich, R.W., Corey, D.P., Stevens, C.F. 1983. A reinterpretation of mammalian sodium channel gating based on single channel recording. *Nature (London)* **306:**436–441
2. Almers, W., McClesky, E.W. 1984. Non-selective conductance in calcium channels of frog muscle: Calcium selectivity in single-file pore. *J. Physiol. (London)* **353:**585–608
3. Armstrong, C. 1981. Sodium currents and gating currents. *Physiol. Rev.* **61:**644–683
4. Barchi, R.L. 1988. Probing the molecular structure of the voltage dependent sodium channel. *Annu. Rev. Neurosci.* **11:**455–489
5. Bossu, J.L., Feltz, A. 1984. Patch-clamp study of the tetrodotoxin-resistent sodium current in group C sensory neurons. *Neurosci. Lett.* **51:**241–246
6. Catterall, W.A. 1988. Structure and function of voltage sensitive ion channels. *Science* **242:**50–61

7. Drews, G., Rack, M. 1988. Modification of sodium and gating currents by amino group specific cross-linking and monofunctional reagents. *Biophys. J.* **54:**383–391
8. Edgar, D., Bard, Y.A., Thoenen, H. 1981. Subpopulations of cultured sympathetic neurons differ in their requirements for survival factors. *Nature (London)* **289:**294–295
9. Fedlova, S.A., Kostyuk, P.G., Vaselovsky, N.S. 1985. Two types of calcium currents in the somatic membrane of newborn rat dorsal root ganglion neurons. *J. Physiol. (London)* **359:**431–446
10. Gilly, W.F., Brismar, T. 1989. Properties of appropriately and inappropriately expressed sodium channel in squid giant axons and its somata. *J. Neurosci.* **9:**1362–1374
11. Gordon, D., Catterall, W.A. 1987. Identification of an intracellular domain of the sodium channel having multiple c-AMP dependent phosphorylation sites. *J. Biol. Chem.* **262:**17530–17535
12. Gordon, D., Merrick, D., Auld, V., Dunn, R., Goldin, A.L., Davidson, N., Catterall, W.A. 1987. Tissue specific expression of the RI and RII sodium channel subtypes. *Proc. Natl. Acad. Sci. USA* **84:**308–313
13. Gordon, R.D., Fieles, W.E., Schotland, D.L., Hogue-Angeletti, R., Barchi, R.L. 1987. Topographical localization of the C-terminal region of the voltage dependent sodium channel from *Electrophorus electricus* using antibodies raised against a synthetic peptide. *Proc. Natl. Acad. Sci. USA* **84:**308–313
14. Gordon, R.D., Li, Y., Fieles, W.E., Schotland, D.L., Barchi, R.L. 1988. Topological localization of a segment of the eel voltage dependent sodium channel primary sequence (AA927-938) that discriminates models of tertiary structure. *J. Neurosci.* **8:**3742–3749
15. Gottman, K., Dietzel, I.D., Lux, H.D., Huck, S., Rohrer, H. 1988. Development of inward currents in chick sensory and autonomic neuronal precursor cells in culture. *J. Neurosci.* **8:**3722–3733
16. Guyton, A.C. 1981. Medical Physiology. Chap. 48. pp. 595. Sounders, Philadelphia
17. Hamill, O.P., Marty, A., Neher, E., Sakman, B., Sigworth, F.J. 1981. Improved patch clamp techniques for high-resolution current recording from cells and cell-free membrane patches. *Pfluegers Arch.* **391:**85–100
18. Harper, A.A., Lawson, J.N. 1985. Conduction velocities related to morphological cell type in rat dorsal root ganglia. *J. Physiol. (London)* **359:**31–46
19. Harper, A.A., Lawson, J.N. 1985. Electrical properties of dorsal root ganglion neurons with different peripheral nerve conduction velocities. *J. Physiol. (London)* **359:**47–63
20. Hess, P., Lansman, J.B., Tsien, R.W. 1986. Calcium channel selectivity for divalent and monovalent cations. *J. Gen. Physiol.* **88:**293–319
21. Heyer, E.J., McDonald, R.L. 1982. Calcium and sodium dependent action potentials of mouse spinal cord and dorsal root ganglion neurons in cell culture. *J. Neurophysiol.* **47:**641–655
22. Hille, B. 1984. Ionic Currents of Excitable Membrane. Sinauer, Sunderland (MA)
23. Hille, B., Woodhull, A.M., Shapiro, B.I. 1975. Negative surface charge near sodium currents of nerve: Divalent ions, monovalent ions and pH. *Phil. Trans. R. Soc. London B* **270:**301–318
24. Hodgkin, A.L., Huxley, A.F. 1952. A quantitative description of membrane currents and its application to conduction and excitation in nerve. *J. Physiol. (London)* **117:**500–544
25. Huang, J.M.C., Tanguy, J., Yeh, J.Z. 1987. Removal of sodium inactivation and block of sodium channels by chloramine-T in crayfish and squid giant axons. *Biophys. J.* **52:**155–163
26. Ikeda, S.R., Schofield, G.G. 1987. Tetrodotoxin resistant sodium current at nodose neurons; monovalent cation selectivity and divalent cation block. *J. Physiol. (London)* **389:**255–270
27. Kameyama, M., Hofmann, F., Trautwein, W. 1985. On the mechanism of beta-adrenergic regulation of the Ca channel in the guinea-pig heart. *Pfluegers Arch.* **405:**285–293
28. Kayano, T., Noda, M., Flockerzi, V., Takahashi, H., Numa, S. 1988. Primary structure of rat brain sodium channel III deduced from the cDNA sequence. *FEBS Lett.* **228:**187–194
29. Kostyuk, P.G., Shuba, Ya.M., Savahenko, A.N. 1988. Three types of calcium currents in the membrane of mouse sensory neurons. *Pfluegers Arch.* **411:**661–669
30. Kostyuk, P.G., Vaselovsky, N.S., Tsynderenko, A.Y. 1981. Ionic currents in the somatic membrane of the rat dorsal root ganglion neurons. I. Sodium currents. II. Calcium currents. *Neuroscience* **6:**2423–2438
31. Krafte, D.S., Snutch, T.P., Leonard, J.P., Davidson, N., Lester, H.A. 1988. Evidence for the involvement of more than one mRNA species in controlling the inactivation process of rat and rabbit brain Na channels expressed in *Xenopus* oocytes. *J. Neurosci.* **8:**2859–2868
32. Lee, K.S., Akaike, N., Brown, A.M. 1977. Trypsin inhibits the action of tetrodotoxin on neurons. *Nature (London)* **265:**751–753
33. Lucas, J.H., Gross, G.W., Tramp, B.F., Balentine, J.D., Berezesky, I.K., Young, W., Gilad, G.M., Bernstein, J.S. 1988. Cellular and molecular correlates of central nervous system trauma. *J. Neurotrauma* **5:**209–258
34. Matsuda, Y., Yoshida, S., Yonezawa, T. 1978. Tetrodotoxin sensitivity and calcium component of action potentials of mouse dorsal root ganglion cell cultured in-vitro. *Brain Res.* **154:**69–82
35. McLean, M.J., Bennet, P.B., Thomas, R.M. 1988. Subtypes of dorsal root ganglion neurons based on different inward currents as measured by whole cell voltage clamp. *Molec. Cell. Biochem.* **80:**95–107
36. Meiri, H., Omri, G., Zeitoun, I., Savion, N. 1986. Environmental factors that influence the differentiation and the development of voltage dependent sodium channels in cultured dorsal root ganglion cells of newborn rats. *Exp. Brain Res.* **13:**231–245
37. Meiri, H., Sammar, M., Schwartz, A. 1989. Production and use of synthetic peptide antibodies to map a region associated with sodium channel inactivation. *Methods Enzymol.* **178:**714–739
38. Meiri, H., Spira, G., Sammar, M., Namir, M., Schwartz, A., Komoriya, A., Kosower, E.M., Palti, Y. 1987. Mapping a region associated with Na channel inactivation using antibodies to synthetic peptide corresponding to a part of the channel. *Proc. Natl. Acad. Sci. USA* **84:**5058–5062
39. Merrifield, R.B. 1965. Solid phase synthesis. *Science* **150:**178–185
40. Messner, D.J., Feller, D.J., Scheuer, T., Catterall, W.A. 1986. Functional properties of rat brain sodium channel lacking the $beta_1$ or $beta_2$ subunits. *J. Biol. Chem.* **26:**14882–14890
41. Meves, H., Rubly, N., Stampfli, R. 1988. The action of argi-

nine-specific reagents on ionic and gating currents of frog myelinated nerve. *Biochem. Biophys. Acta.* **943:**1–12
42. Noda, M., Ikeda, T., Kayano, T., Suzuki, H., Takashima, H., Kuraski, M., Takahashi, H., Nakayama, H., Numa, S. 1986. Existence of distinct sodium channel messenger RNAs in rat brain. *Nature (London)* **320:**188–192
43. Noda, M., Shimizu, S., Tannabe, T., Takai, T., Kayano, T., Ikeda, T., Takahashi, H., Nakayama, H., Kanaoka, Y., Miniamino, N., Kangawa, K., Matsuo, H., Raftery, M.A., Miyata, T., Numa, S. 1984. Primary structure of electrophorus sodium channel deduced from c-DNA sequence. *Nature (London)* **312:**121–127
44. O'Dowd, D.K., Ribera, A.B., Spitzer, N.C. 1987. Development of voltage-dependent calcium, sodium and potassium currents in *Xenopus* spinal neurons. *J. Neurosci.* **8:**792–805
45. Okun, L.M. 1972. Isolated dorsal root ganglion neurons in culture: Cytological maturation and extension of electrically active processes. *J. Neurobiol.* **3:**111–151
46. Omri, G., Meiri, H. 1990. Characterization of sodium currents in mammalian sensory neurons cultured in serum-free defined medium with and without NGF. *J. Membrane Biol.* **115:**13–29
47. Orozco, C.B., Epstein, C.J., Rapoport, S.I. 1988. Voltage activated sodium conductance in cultured normal and trisomy-16 dorsal root ganglion neurons from fetal mouse. *Dev. Brain Res.* **3:**265–274
48. Oxford, G.S. 1978. Removal of sodium channel inactivation in squid giant axons by N-bromoacetamide. *J. Gen. Physiol.* **71:**227–247
49. Palti, Y., Cohen-Armon, M. 1982. Numerical method for correcting the series resistance error in voltage clamp experiments. *Isr. J. Med. Sci.* **18:**19–24
50. Papazian, D.M., Schwartz, T.L., Temple, B.L., Jan, Y.N., Jan, L.Y. 1984. Cloning of genomic and complimentary DNA from shaker a putative potassium channel gene from *Drosophila*. *Science* **237:**749–753
51. Purves, D., Lichtman, J.W. 1985. Principles of Neuronal Development. Chapter 7. Trophic effects of targets on neurons. pp. 155–178. Sinauer, Sunderland (MA)
52. Rojas, E., Rudy, B. 1976. Destructive of the sodium conductance inactivation by a specific protease in perfused nerve fibers from *Loligo*. *J. Physiol. (London)* **262:**501–531
53. Sackmann, B., Methfessel, C., Mishina, M., Takahashi, T., Takai, T., Kuraski, M., Fukuda, K., Numa, S. 1985. Role of acetycholine receptor subunits in gating of the channel. *Nature (London)* **318:**538–543
54. Schmidt, J., Rossie, S., Catterall, W.A. 1985. A large intracellular pool of inactive Na channel alpha subunits in developing rat brain. *Proc. Natl. Acad. Sci. USA* **82:**4847–4851
55. Scott, B.S., Edwards, B.A.V. 1980. Electric membrane properties of adult mouse DRG neurons and the effect of culturing duration. *J. Neurobiol.* **11:**291–301
56. Spalding, B.C. 1980. Properties of toxin resistant sodium channels produced by chemical modification in frog skeletal muscles. *J. Physiol. (London)* **305:**485–500
57. Spitzer, N.C. 1979. Ion channels in development. *Annu. Rev. Neurosci.* **2:**363–397
58. Stolc, S., Nemcek, V., Boska, D. 1988. Potential clamp of isolated dialyzed neuron: Minimalization of the effect of series resistance. *Gen. Physiol. Biophys.* **7:**303–312
59. Stuhmer, W., Conti, F., Suzuki, H., Wang, X., Noda, M., Numa, S. 1989. Structural parts involved in activation and inactivation of the sodium channel. *Nature (London)* **339:**597–603
60. Tanabe, T., Takeshima, H., Mikawi, A., Flocherzi, V., Takahashi, H., Kangawa, K., Kayima, M., Matsuo, H., Hirose, T., Numa, S. 1987. Primary structure of the receptor for calcium channel blockers from skeletal muscle. *Nature (London)* **328:**313–318
61. Trimmer, S., Jr., Cooperman, S.S., Tomiko, S.A., Zhou, J., Crean, S.M., Boyk, M.B., Galle, R.G., Sheng, Z., Barchi, R.L., Sigworth, F.J., Goodman, R.H., Agnew, W.S., Mandel, G. 1989. Primary structure and functional expression of a mammalian skeletal muscle sodium channel. *Neuron* **3:**33–49
62. Vassilev, P.M., Scheur, T., Catterall, W.A. 1988. Identification of an intracellular peptide segment involved in sodium channel inactivation. *Science* **241:**1658–1661
63. Weiss, R.E., Horn, R. 1986. Functional differences between two classes of sodium currents in developing rat skeletal muscle. *Science* **233:**361–364
64. Yoshida, S., Matsuda, Y., Samejima, A. 1978. Tetrodotoxin-resistant sodium and calcium component of action potentials in DRG cells of the adult mouse. *J. Neurophysiol.* **41:**1096–1106
65. Zeitoun, I., Meiri, H., Omri, G., Palti, Y. 1987. The development of different types of Na channels in rat DRG cells. *Proc. Int. Biophys. Cong.* **9:**143

Received 17 August 1989; revised 2 January 1990